

RESULTS FROM HIGH ENERGY PHOTOPRODUCTION  
AT THE CERN SPS

F. Richard  
Laboratoire de l'Accélérateur Linéaire  
91405 - Orsay, FRANCE

SUMMARY

We present results from a photoproduction experiment using the CERN  $\Omega$  spectrometer with a tagged photon beam giving energies between 20 and 70 GeV. Charm physics and vector meson searches are emphasized. A luminosity of 80 events/nb was obtained on events with a detected charged kaon and of 60 events/nb on events with at least four prongs. Results on an emulsion exposure using the same apparatus are also presented.

INTRODUCTION

I will discuss high energy photoproduction at CERN. Since August 1977 a British-French-German collaboration has been collecting data with the CERN spectrometer in a tagged photon beam in the West Area (WA4 experiment). The data taking has been completed in April 1978 and final analysis in April 1979. My talk will cover the work of WA4 on vector mesons and charm physics.

In the same apparatus, an experiment was carried out in collaboration with an emulsion group\*\* to measure the charm lifetime. I will report on a charm candidate found in this experiment.

The set up

1) Tagged photon beam

Fig. 1 shows the principle of this beam. A 210 GeV proton beam hits a beryllium target producing a neutral beam. Photons are converted into electrons in a .5 radiation length lead radiator. The electrons, transported at a mean momentum of 81 GeV  $\pm$  2 %, are individually measured in a set of MWPC. After production of a bremsstrahlung photon beam in a 7.6 % radiation length tungsten radiator the electrons are detected in a system of proportional chambers, counter hodoscopes and lead glass counters.

The tagged photons have an energy range from 20 to 70 GeV and are measured to an accuracy of  $\pm$ 300 MeV. A typical photon flux was  $2 \cdot 10^5$ /s. The pion contamination in the electron beam is  $\sim$  2 %.

2) Detector

The  $\Omega$  spectrometer shown in Fig.2 has a magnetic field which gives 3 T - m from the hydrogen target to the drift chambers. In addition to the spark chambers which are viewed by Plumbicon cameras<sup>1</sup>, four proportional chambers plus two drift chambers are used to improve the measurement accuracy and to trigger the system.

Particles are identified in a threshold Cerenkov counter divided into 32 cells and filled with CO<sub>2</sub> at atmospheric pressure. Effective thresholds are 5.5 GeV

\* Bonn, CERN, Ecole Polytechnique, Glasgow, Lancaster, Manchester, Orsay, Paris VI, Paris VII, Rutherford, Sheffield.

\*\* Bologna, CERN, Firenze, Genova, Lebedev Institute Moscow, Paris VI, Santander, Valencia.

for pions and 18 GeV for Kaons. The photon detector consists of a mosaic of 340 lead glass blocks of 14 x 14 cm<sup>2</sup>. It covers roughly an acceptance cone of 120 mrad aperture. Photons are converted in an active converter of 3 radiation length of lead glass and their coordinates are measured in two planes of 960 scintillator bars. All the elements of the detector are individually recorded by ADC's.

3) Trigger

An open trigger is clearly excluded by the high electromagnetic cross section of 20 mb and the dead time (20 ms) limitation of the  $\Omega$  spark chamber read-out system. We required a multiplicity between 4 and 9 at a plane 1.60 m downstream of the center of the target. The 67 cm long hydrogen target is surrounded by a cylindrical hodoscope of 24 slabs closed by a proportional chamber with .5 mm wire spacing. A multiplicity of at least 4 was also demanded at this level.

6.1 M triggers have been recorded. About 70 % of the multiplicity trigger data presented here were obtained with above requirements while for the remainder we required in addition, through a logic matrix, a charged kaon in the final state. Special triggers were used for two prongs  $K^+K^-$  and  $p\bar{p}$ . A sample of  $\pi^+\pi^-$  events is also available but with reduced luminosity.

4) Sensitivity

Multiplicity data with a charged K or proton in the final state and  $K^+K^-$  ( $p\bar{p}$ ) data have a luminosity of 80 events/nb, while ordinary multiplicity data have 60 events/nb.

I. EXCLUSIVE PHOTOPRODUCTION

A. General remarks

One is primarily interested in heavy vector mesons, presumably  $q\bar{q}$  radial excitations<sup>2</sup>, which couple diffractively to the photons.

Obvious criteria to define such objects are :

- Steep t dependence  $\sim e^{-5t}$
- Weak energy dependence
- Pure spin parity  $J^P = 1^-$  state.

Broad enhancements, .5 GeV wide, can be produced by a Deck-type mechanism. This effect creates mixed parity states, so that one can hope to discriminate against them.

For diffractively produced events, the majority of the recoil protons stop in the target or fall outside the accepted angular region. We therefore selected events of net charge 0 or 1, balancing the energy of the incident photon to  $\pm$  1 GeV. Using fully reconstructed events, about 30 % of the total, we estimated the inelastic contamination for each channel. In all cases, it fell below 30 %.

Since vector mesons are produced conserving s channel helicity, we choose for the quantization axis

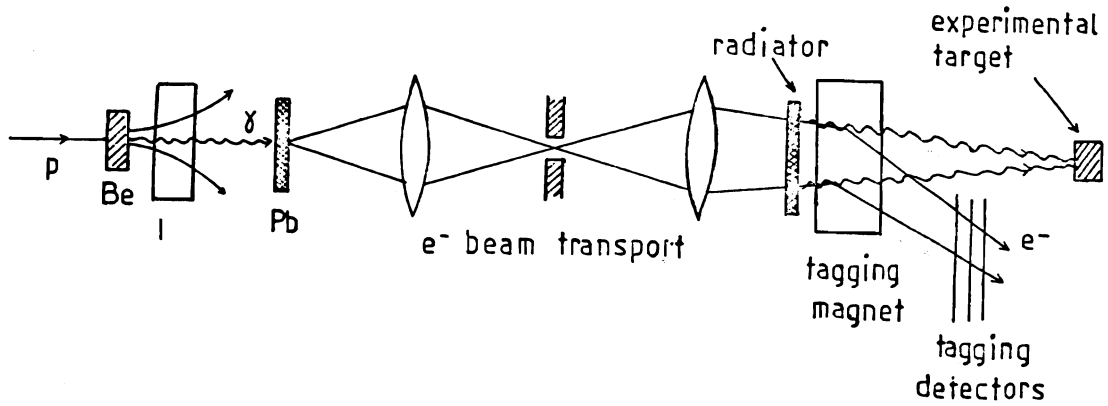
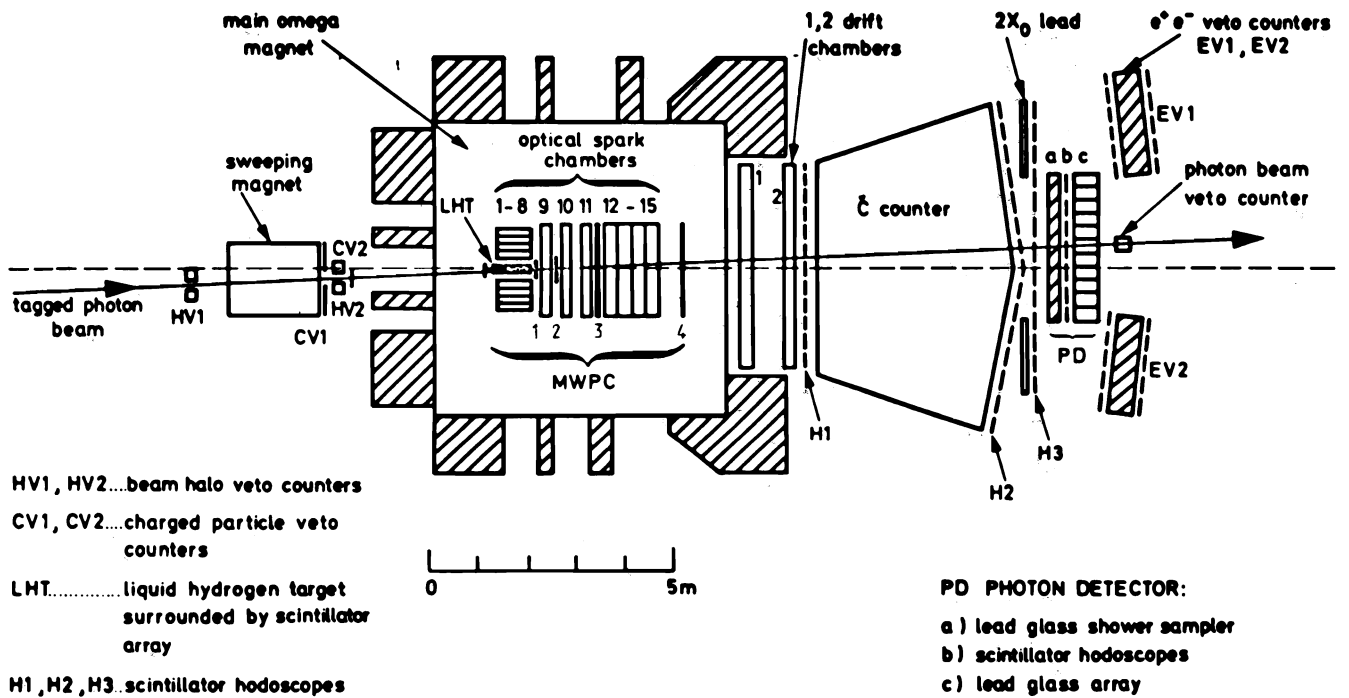


Fig. 1. Schematic view of the tagged photon beam.



LAYOUT OF THE OMEGA SPECTROMETER FOR PHOTOPRODUCTION EXPERIMENTS

Fig. 2. The Omega Spectrometer.

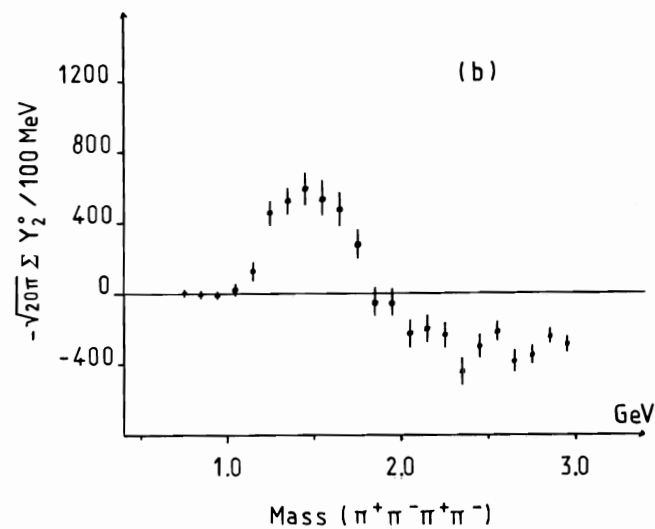
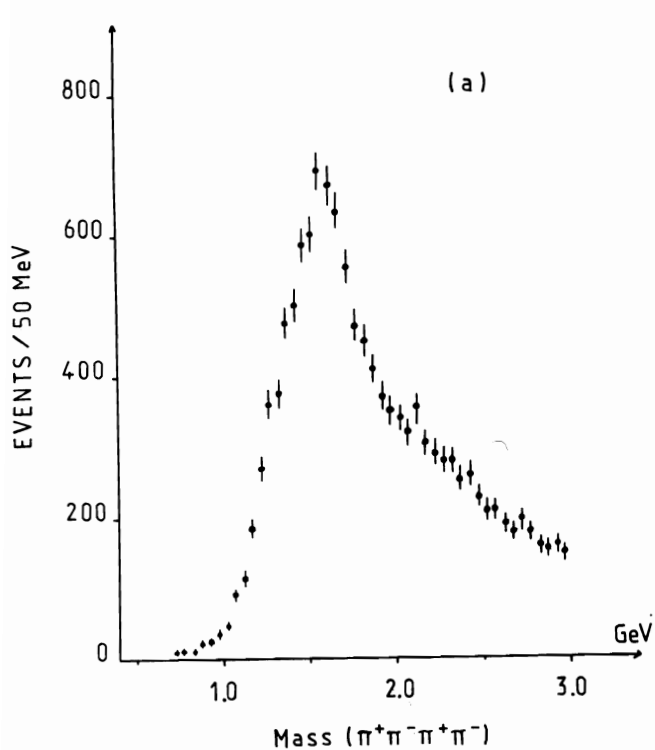


Fig. 3. (a)  $4\pi$  mass spectrum in  $\gamma p \rightarrow \pi^+ \pi^- \pi^+ \pi^- p$   
 (b)  $-\sqrt{20\pi} \langle Y_2^0(\theta_{++}) \rangle$  distribution where  $\theta_{++}$  is the angle between the resultant of the momenta of the two  $\pi^+$  mesons and the  $4\pi$  direction in the CM-system

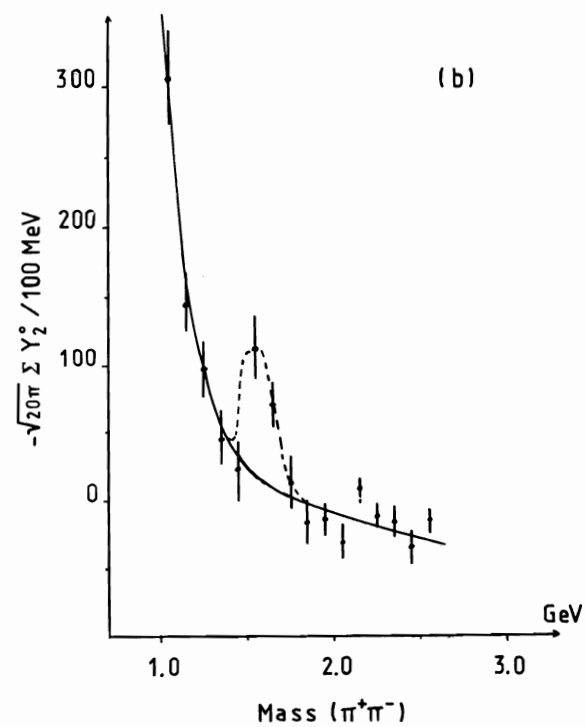
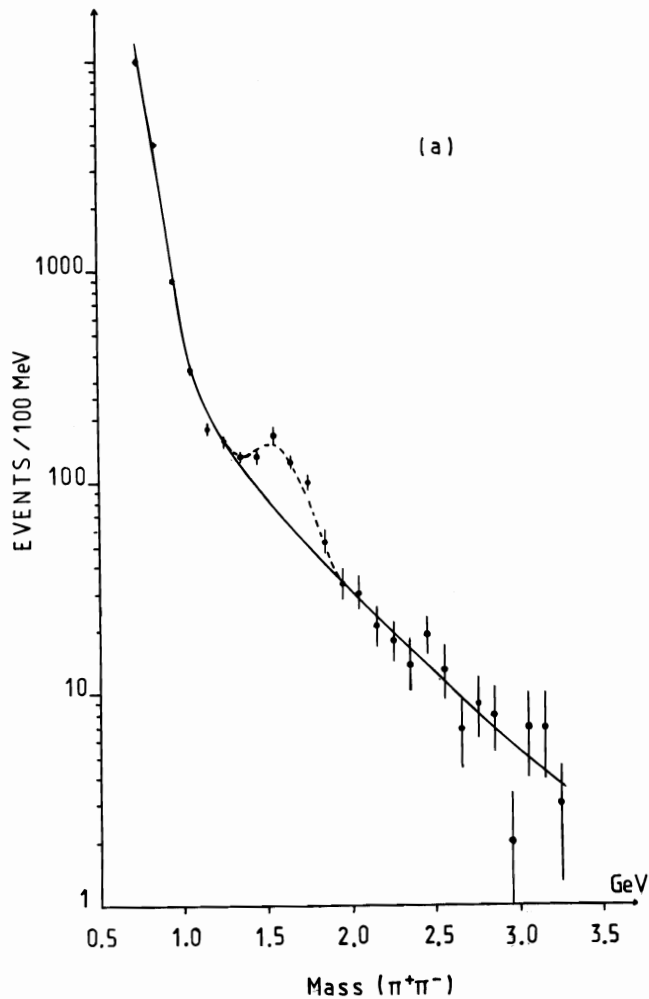


Fig. 4. (a)  $2\pi$  mass distribution in  $\gamma p \rightarrow \pi^+ \pi^- p$   
 (b)  $-\sqrt{20\pi} \langle Y_2^0(\theta) \rangle$  distribution where  $\theta$  is the angle between the momentum of a  $\pi$  meson and the  $\pi^+ \pi^-$  direction in the CM-system.

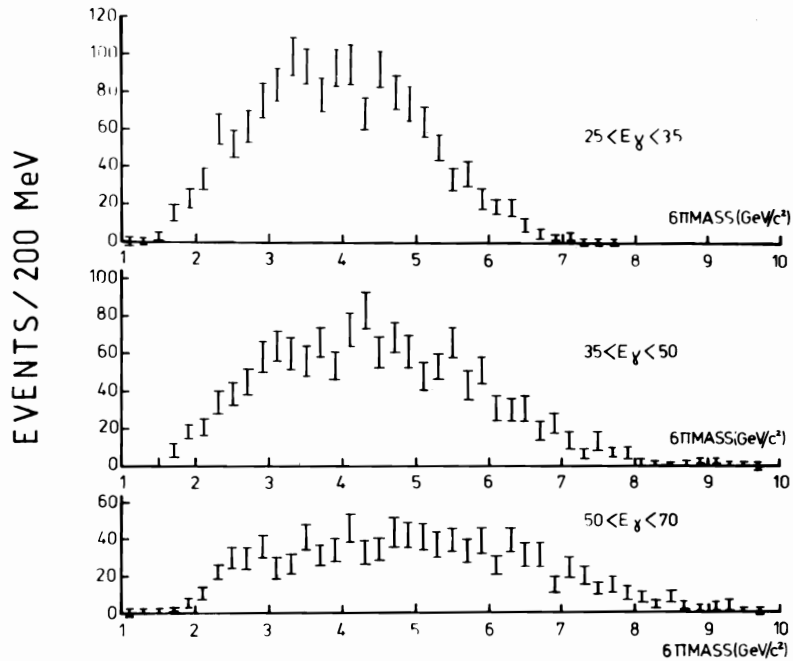
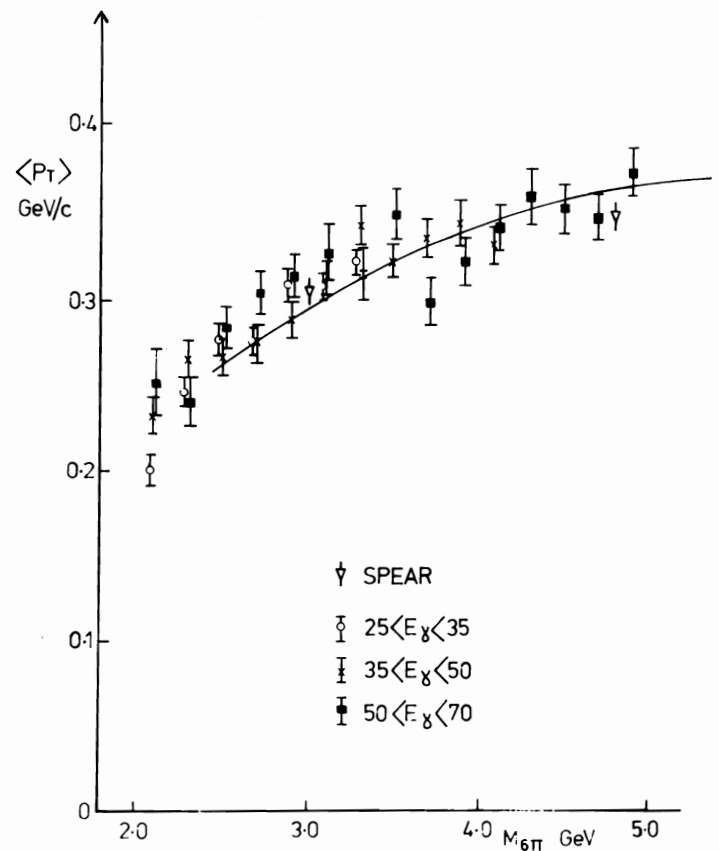


Fig. 5.  $6\pi$  mass distribution in  $\gamma p \rightarrow \pi^+\pi^-\pi^+\pi^-\pi^+\pi^-p$  for three different ranges of photon energy.

Fig. 6. Experimental values of  $\langle p_T \rangle$ , the average of  $p_T$  of the six pions with respect to the photon direction in the  $6\pi$  rest system, as a function of mass of the  $6\pi$  system, for three ranges of incident photon energy. The curve corresponds to a  $p_T$  truncated phase space distribution.



the direction of the vector meson in the center of mass of the reaction :  $\gamma p \rightarrow V\rho$ . As in the well known case of  $\rho' (1600) \rightarrow 4\pi$ , one usually defines subsystems or resonances to reduce the angular analysis to a two body decay distribution with respect to the s channel axis.

## B. Pion channels

### 1. $\pi^+ \pi^- \pi^+ \pi^-$ , high mass $\pi^+ \pi^-$ .

At low  $4\pi$  masses a structure centered at 1.6 GeV, .5 GeV wide, is clearly visible (Fig. 3). It has the following properties :

- cross section  $0.8 \pm .3 \mu\text{b}$
- average t slope  $6 \text{ GeV}^{-2}$
- probability of 0.9 to find a  $\rho$  in one of the  $4 \pi^+ \pi^-$  combinations.

Using  $\vec{\pi}^+ + \vec{\pi}^+$ , the sum of momenta of positive pions, as an analyzer, we find that  $\langle Y_2^0(\cos \theta_{++}) \rangle$  distribution of Fig. 3b is consistent with the  $J^P = 1^-$  hypothesis.

The  $\langle Y_2^0 \rangle$  shape shows we do not have a pure  $1^-$ , but from the fast turn over observed at 1.8 GeV, which indicates some cancellation from the non resonant component and from the limited efficiency of the analyzer, one can assume that the bump is consistent with being a pure  $1^-$ .

The channel  $\gamma p \rightarrow \pi^+ \pi^- p$  shows a similar structure at 1600 GeV compatible with  $J^P = 1^-$  (Fig. 4) but possibly narrower ( $\Gamma = 0.23 \pm .08 \text{ GeV}$ ). Since the two channels may have a substantial non resonant component, interference effects could explain this discrepancy.

This  $\pi^+ \pi^-$  mode has a cross section of  $130 \pm 20 \text{ nb}$  with a branching ratio  $\rho' \rightarrow 2\pi/\rho' \rightarrow \pi^+ \pi^- \pi^+ \pi^-$  of  $.16 \pm .05$ .

For  $4\pi$  masses greater than 2 GeV there is  $\sim 0.5 \rho/\text{event}$ . The t-distribution remains peripheral with a slope of  $\sim 5$ . The data are consistent with a  $P_{\perp}$  truncated phase space (see § on  $6\pi$ ).

### 2. $\pi^+ \pi^- \pi^+ \pi^-$ .

No structure is visible in the mass distribution (Fig. 5). There is a weak  $\rho$  component ( $\rho/\pi \sim .1$ ). We have used this reaction to study the dynamics of diffractive photoproduction for high masses.

To isolate the  $6\pi$  diffractive component in the absence of a recoil proton identification is non trivial. However, and this has been thoroughly investigated by Monte-Carlo calculations, it can be done provided one eliminates masses higher than  $.5 \text{ s}^{1/2}$ .

A detailed analysis of these data shows that the various observables  $P_{\perp}$ , y, x can be reproduced by a  $P_{\perp}$  truncated phase space,  $P_{\perp}$  being defined with respect to the photon axis. The whole picture thus seems consistent with the conventional V.D.M. picture of the  $\gamma$  behaving like a  $\rho$ . However, since there is no strong leading  $\rho$  component for  $4\pi$  and  $6\pi$ , one can as well describe the process as the  $\gamma$  materializing in a qq pair with subsequent dressing into jets. To reproduce the data, this qq needs to be produced lined along the initial  $\gamma$ .

Fig. 6 shows that the  $\langle P_{\perp} \rangle$  obtained in our data agrees well with that which is found at Spear, supporting the quark picture.

### 3. $\pi^+ \pi^- \pi^0$

The mass distribution is shown in Fig. 7 for masses above the  $\omega$ . A  $\phi$  is clearly seen but also there are indications of enhancements centered at 1.27 and 1.67 GeV, with widths of about 100 MeV. From comparing with the  $\omega$ , one obtains a cross section of  $\sim 100 \text{ nb}$  for each structure. From the  $\rho^0$  and  $\rho^{\pm}$  spectra associated to this region of mass, it seems that the channel is dominated by  $\rho\pi$ .

To assign unambiguously the quantum numbers ( $J^P$ , I) of these objects requires more statistics than we have.

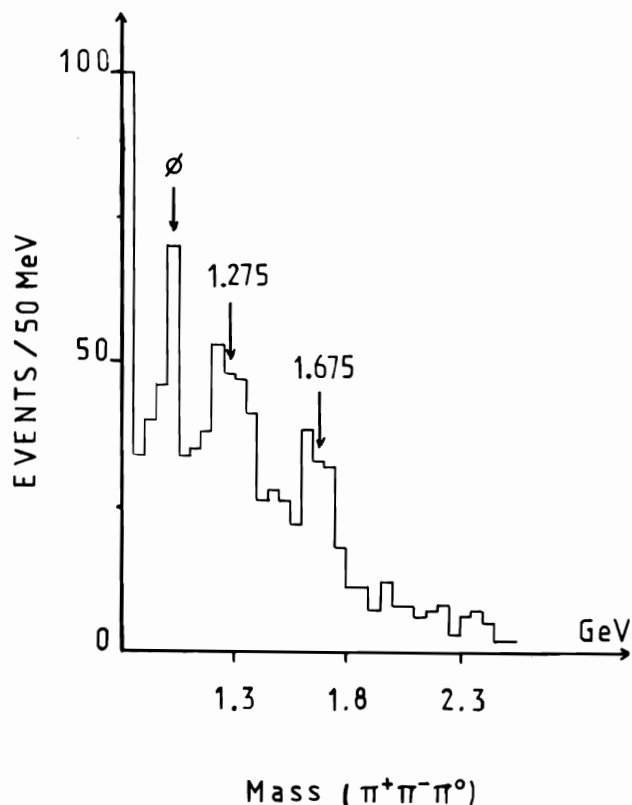


Fig. 7 :  $3\pi$  mass distribution in  $\gamma p \rightarrow \pi^+ \pi^- \pi^0 p$  above the  $\omega$  mass.

### 4. $\pi^+ \pi^- \pi^0 \pi^0$

The mass distribution (Fig. 8a) shows a structure centered at 1.25 GeV, .4 GeV wide, which is primarily related to the  $\omega\pi^0$  contribution (I = 1 system). The cross section is  $\sim 1 \mu\text{b}$ . This enhancement has been observed indirectly in previous experiments<sup>3,4</sup> but the results were equally consistent with  $J^P = 1^+$  and  $1^-$  and the state was not definitely established as  $\omega\pi^0$ . From the angular distribution (Fig. 8c) of the normal to the  $\omega$  plane, we conclude that we are dealing with a mixed spin parity with  $1^-$  dominant. The interpretation of the entire enhancement as the  $1^+B$  meson is ruled out.

In conclusion, the data favor a vector state, however we are unable to determine whether that state is a resonance, and hence a recurrence of the  $\rho$ , or a non-resonant threshold effect.

$$\gamma p \rightarrow \pi^+ \pi^- \pi^0 \pi^0 p$$

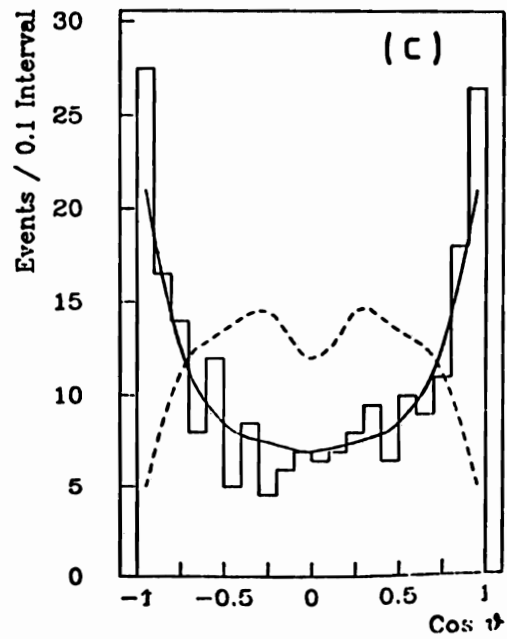
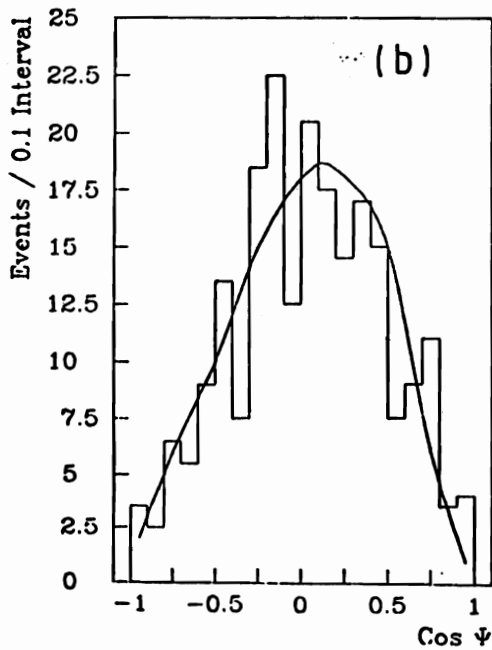
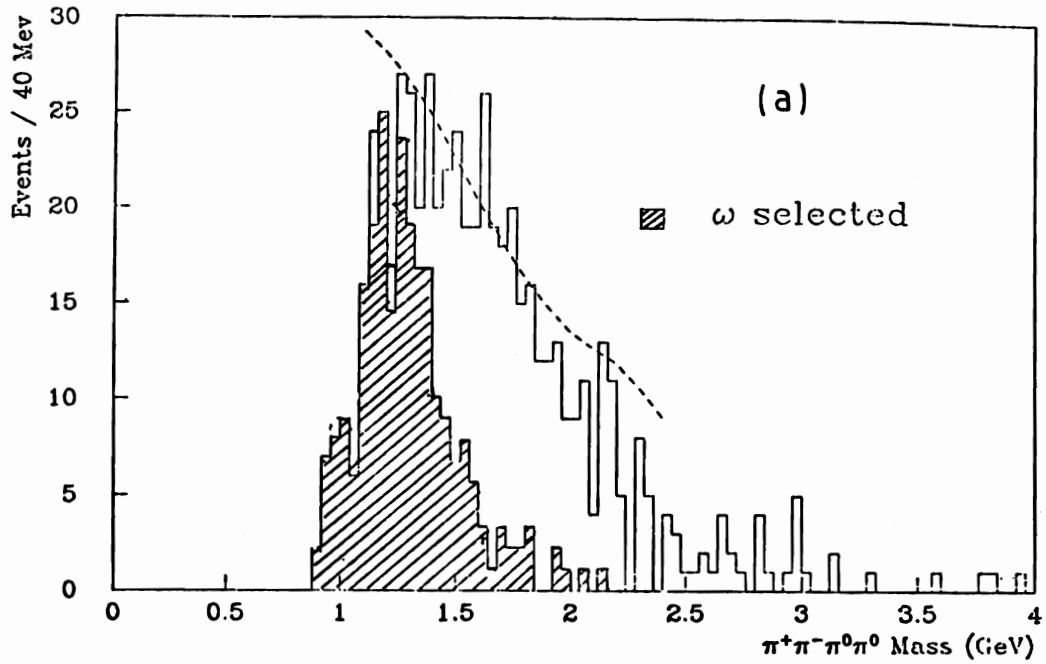


Fig. 8. (a)  $\pi^+ \pi^- \pi^0 \pi^0$  mass spectrum for the channel  $\gamma p \rightarrow \pi^+ \pi^- \pi^0 \pi^0 p$ . The shaded area shows the  $\pi^+ \pi^- \pi^0 \pi^0$  mass spectra for events containing a  $\pi^+ \pi^- \pi^0$  combination with mass in the range  $0.72 - 0.84 \text{ GeV}/c^2$ . The solid line shows the acceptance for the  $\omega \pi^0$  system averaged over energy.

(b) - (c) Polar decay angles  $\psi$  and  $\theta$  for the  $\omega$  in the  $\omega \pi^0$  rest frame and the  $\omega$  normal respectively. The solid curve gives the acceptance biased angular distribution for an isotropically decaying  $\omega \pi^0$  system. The dashed curve shows the expected distribution for the decay of a  $1^+$  object.

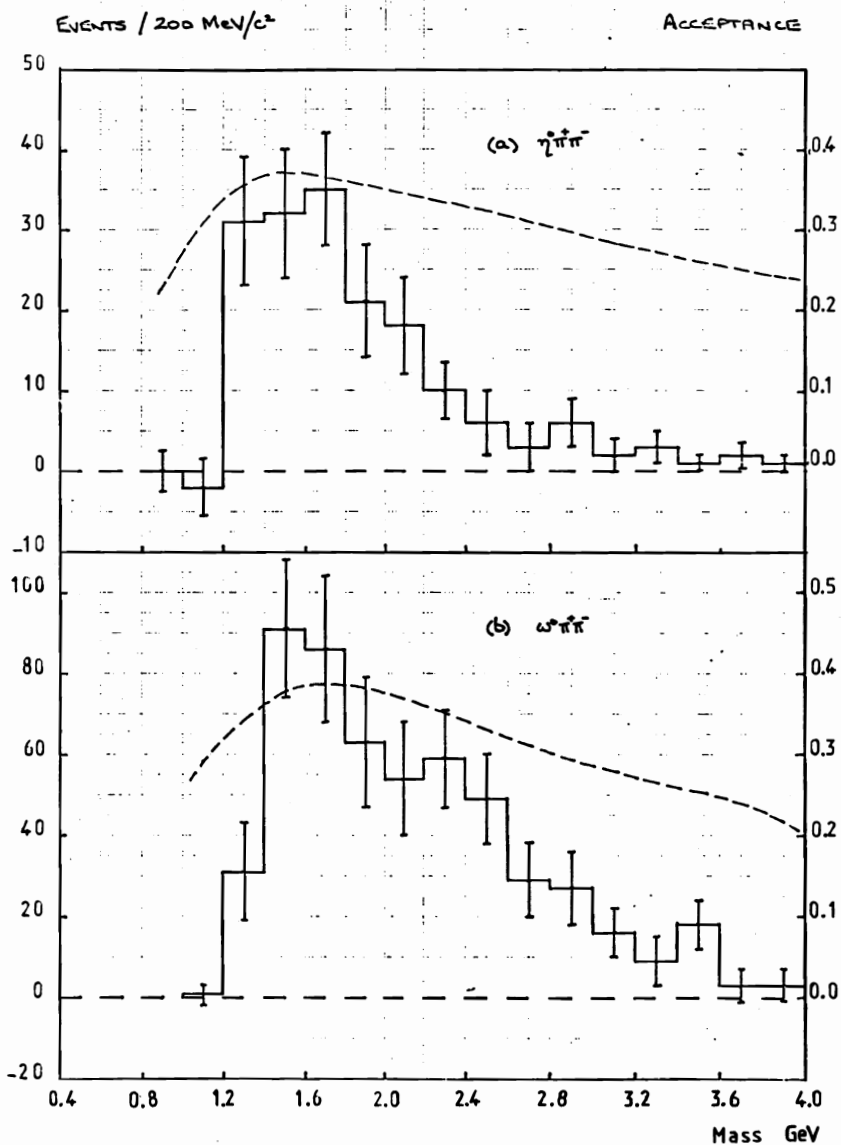


Fig. 9.  $5\pi$  mass distributions in  $\gamma p \rightarrow \pi^+ \pi^- \pi^+ \pi^- \pi^0 p$  :  
 (a) for  $\eta^0 \pi^+ \pi^-$   
 (b) for  $\omega^0 \pi^+ \pi^-$   
 Peak-wings subtractions have been done to select  $\eta^0$  and  $\omega^0$ .  
 The curves are acceptances for our detector system.

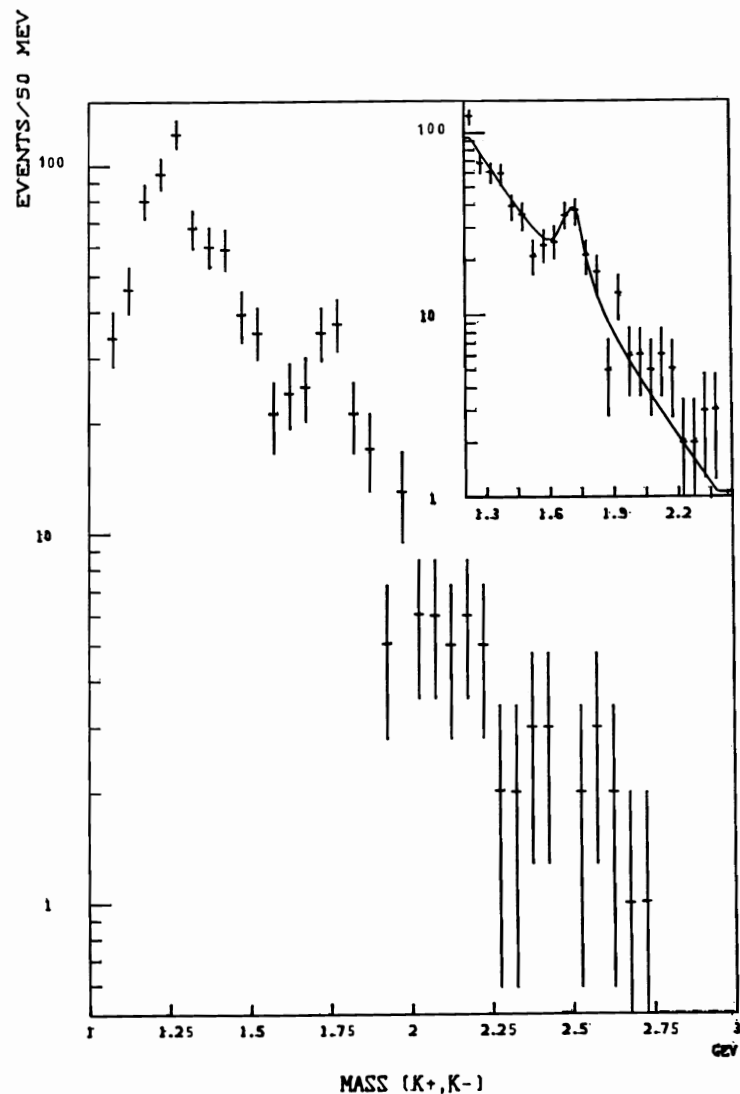


Fig. 10.  $K^+ K^-$  mass distribution in  $\gamma p \rightarrow K^+ K^- p$  above the  $\phi$ .  
 The data are fitted by a gaussian on top of an exponentially falling background. It gives a mass of  $1.76 \pm .01$  GeV and a width of  $120 \pm 30$  MeV.

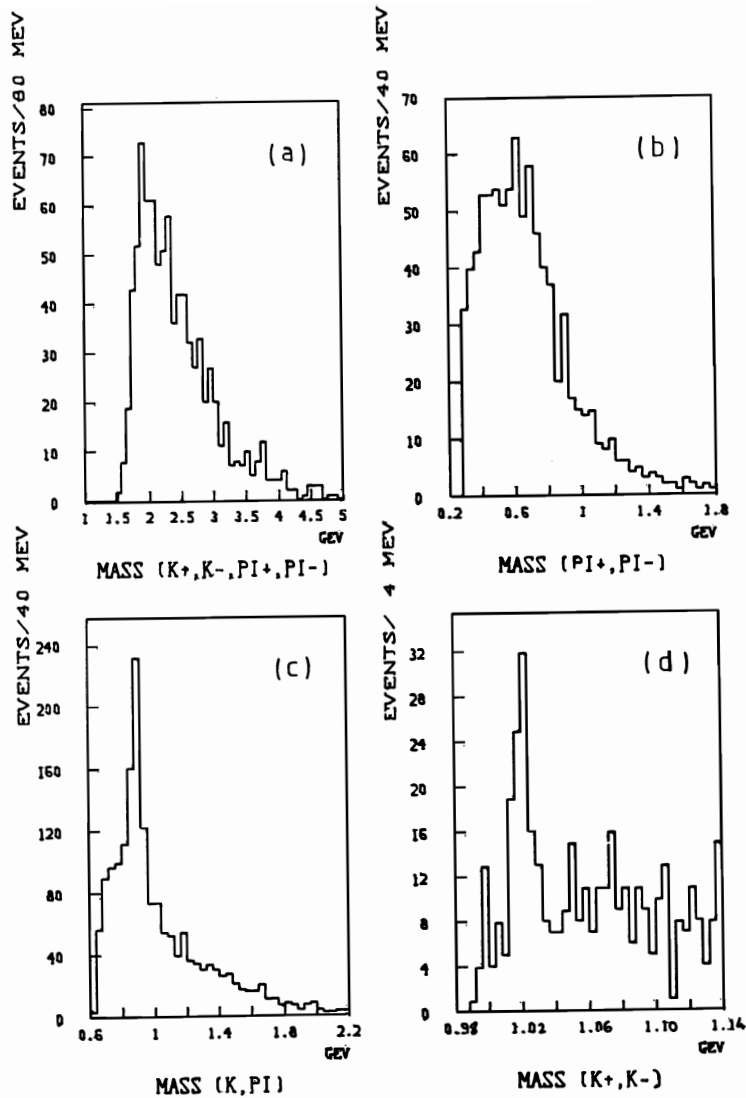


Fig. 11. Mass spectra for the channel  $\gamma p \rightarrow K^+ K^- \pi^+ \pi^-$ .  
 (a)  $K^+ K^- \pi^+ \pi^-$  (b)  $\pi^+ \pi^-$   
 (c)  $K^\pm \pi^\mp$  (d)  $K^+ K^-$

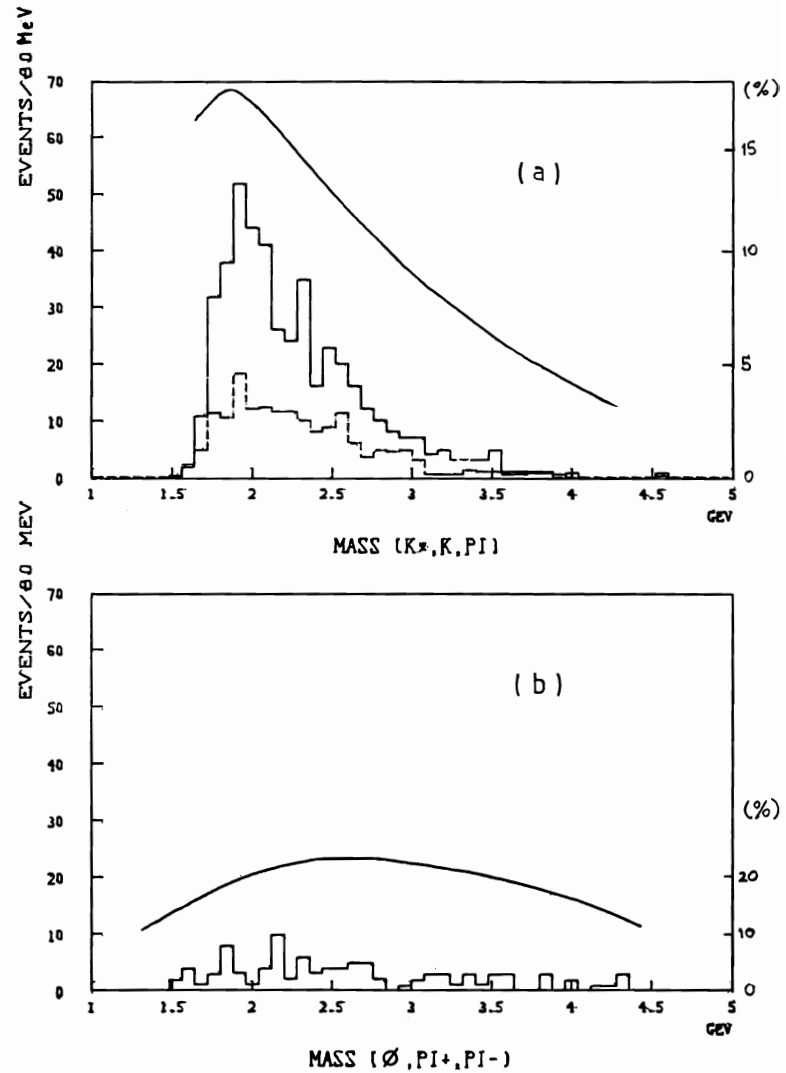


Fig. 12. Mass spectra for the channel  $\gamma p \rightarrow K^+ K^- \pi^+ \pi^- p$  with  $|t| < 0.4 \text{ GeV}^2$ .  
 (a)  $K^* K \pi$  mass spectrum with  $0.83 < M_{K^\pm \pi^\mp} < 0.95 \text{ GeV}$ . The dashed histogram is taken for:  $0.71 < M_{K^\pm \pi^\mp} < 0.83 \text{ GeV}$  and  $0.95 < M_{K^\pm \pi^\mp} < 1.07 \text{ GeV}$ .  
 (b)  $\phi \pi^+ \pi^-$  mass spectrum. The curves are acceptance for our detector system.



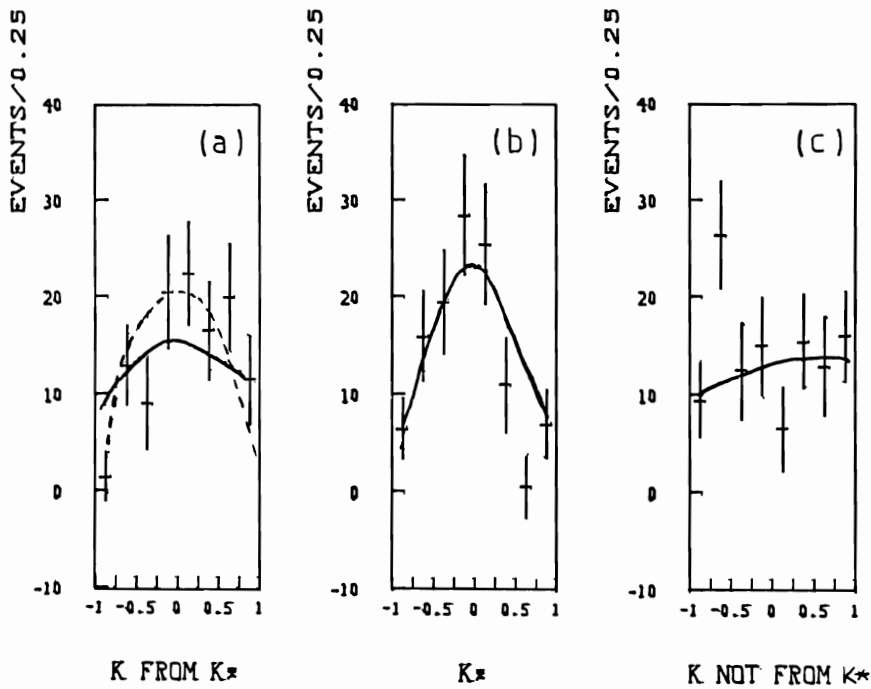


Fig. 13. Polar decay angles for the  $KK\pi\pi$  mass region  $1.8 < M_{KK\pi\pi} < 2.1\text{GeV}$  with  $|t| < 0.4\text{ GeV}^2$ .  
 (a) The K from  $K^*$  (890) decay in the  $K^*$  (890) rest frame ;  
 (b) The  $K^*$  in the  $K^*K\pi$  rest frame ;  
 (c) The K not originating from the  $K^*(890)$  in the  $K\pi$  rest frame.  
 The solid line shows the angular distribution expected for isotropic decay of the  $KK\pi\pi$  system while the dotted line shows the distribution expected from the  $\phi^-(J^P = 1^-)$  decay.

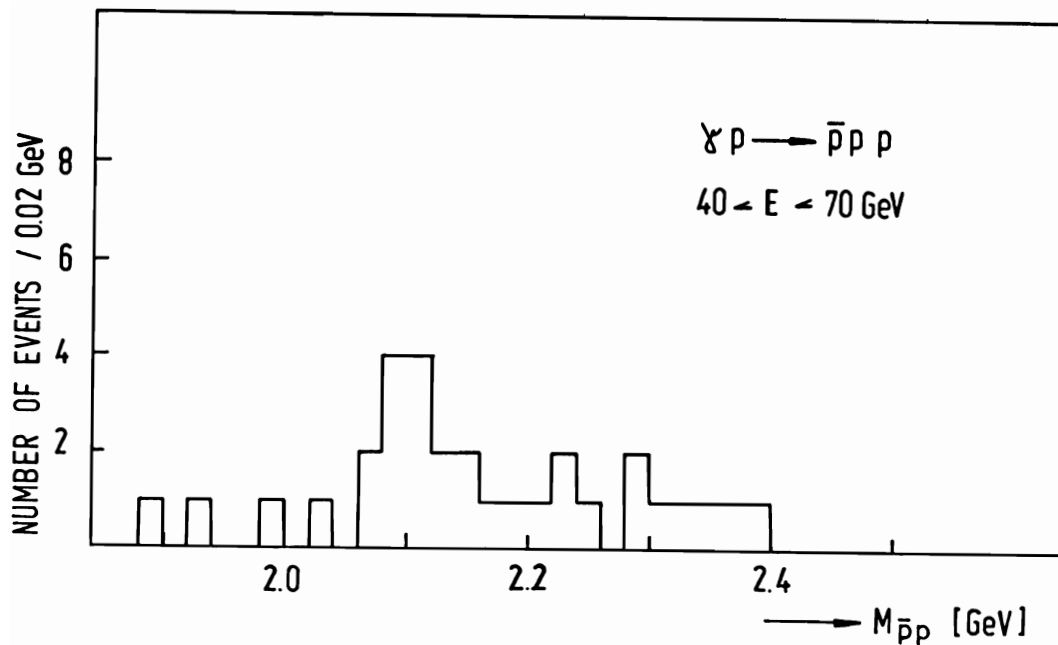


Fig. 14.  $p\bar{p}$  mass distribution in  $\gamma p \rightarrow p\bar{p}p$ .

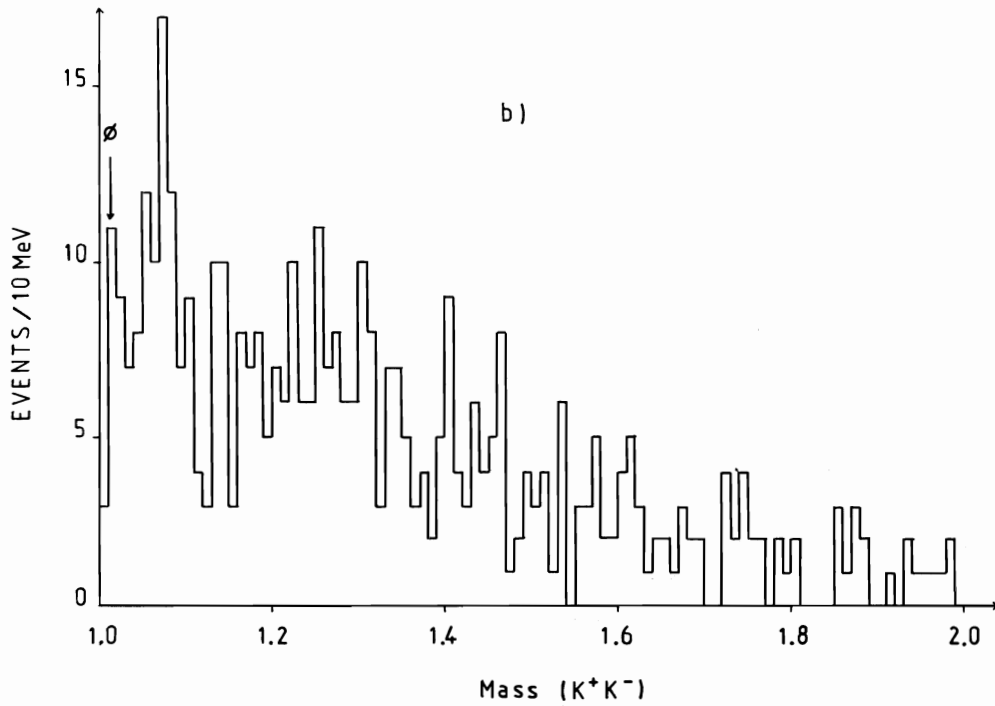
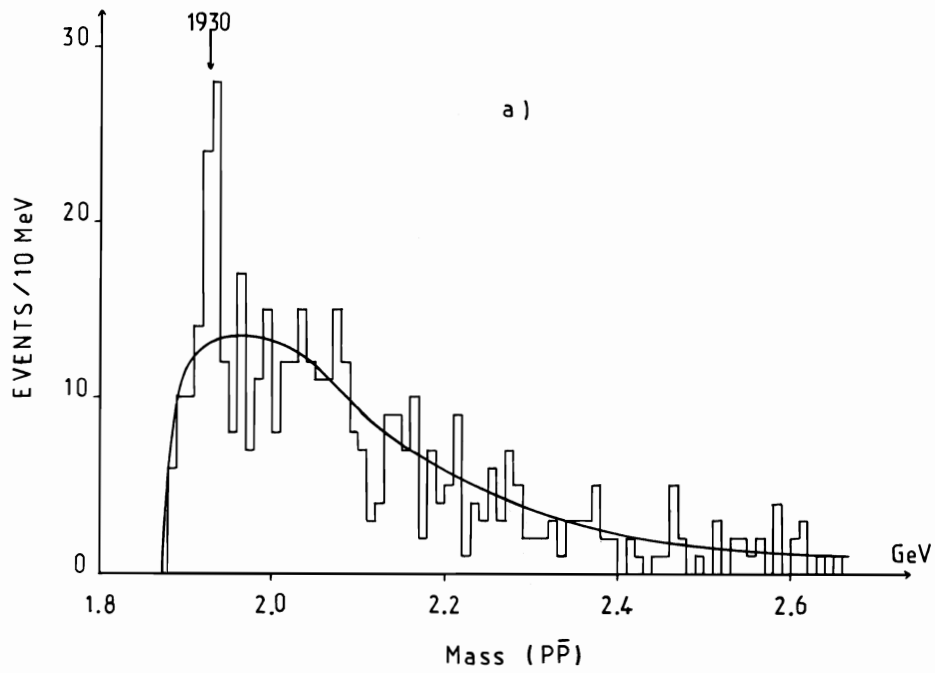


Fig. 15.  $p\bar{p}$  mass distribution in  $\gamma p \rightarrow p\bar{p} + X$  with more than one prong in X.

(a) normal mass assignment.

(b) with the  $K^+K^-$  mass assignment .

5.  $\pi^+ \pi^- \pi^+ \pi^- \pi^0$

This channel, as well as the  $6\pi$  and the high mass  $4\pi$ , appears structureless and seems dominated by the  $P_1$  truncated phase space component. In the sub-masses,  $\omega$  (20 % probability) and  $\eta$  are clearly visible with  $\eta\pi\pi/\omega\pi\pi \sim 1$ .

Selecting these channels by a peak minus wings subtraction we obtain broad threshold enhancements (Fig. 9) analog to the  $\rho^0 \pi^+ \pi^-$  of § 1. Finer binning does not reveal any narrow structure.

C. Kaon channels

Charged kaons are identified between 5.6 GeV and 18 GeV. The Cerenkov inefficiency, studied using  $\rho$  events, is below 2 %.

1.  $K^+ K^-$

The  $\phi$  has the following properties :

$$B_{K^+K^-} \sigma_\phi = (226 \pm 6) \text{ nb} \pm 16 \text{ nb} \text{ syst. error}$$

$$t \text{ slope} = (5.5 \pm 1.2) \text{ GeV}^{-2}$$

for  $20 < E_\gamma < 36 \text{ GeV}$ .

It follows a  $\sin^2 \theta$  law consistent with the  $1^-$  properties.

To increase the acceptance ( $\times 3$ ) in the high mass region, we have used elastic events in which only one of the charged kaons is explicitly signed (no light in the Cerenkov). With 2 % Cerenkov inefficiency, one becomes sensitive to the  $\rho$  contribution (Fig. 10). A structure at  $(1.76 \pm .01) \text{ GeV}$ , 100 MeV wide, is visible. From the size of the  $\rho$  reflexion and from the  $\pi^+ \pi^-$  spectrum shown in § 1B we infer a small  $\pi^+ \pi^-$  contamination in this region of mass. The cross section would be a few nb. This small cross section seems consistent with the fact that such an object has not been observed up to now in photoproduction.

2.  $K^+ K^- \pi^+ \pi^-$

Events are selected by requiring two charged kaons identified by the Cerenkov. The reaction  $\gamma p \rightarrow p p \pi^+ \pi^- p$  may simulate this channel. Using the five prong events, we estimate a 20 % contamination.

The  $KK\pi\pi$  mass spectrum is shown in Fig. 11 together with the relevant submasses. The observed broad threshold enhancement is primarily due to the strong  $K^*$  component (30 %) while  $\phi\pi\pi$  (10 %) shows a phase space like behaviour (Fig. 12). The data in Fig. 12 suggest the existence of a  $K^*K$  object of mass 1.9 GeV, .4 GeV wide, together with some smooth background. In the  $K^+ K^- \pi^+ \pi^-$  mode, it has a cross section of  $60^{+30}_{-20}$  nb. The  $t$  distribution,  $e^{-5t}$ , and the energy dependence are consistent with diffraction.

The decay angular distributions (Fig. 13) are consistent with a  $1^-$  object decaying into  $K^*K\pi$  with the  $K^*$  in a relative S-wave with respect to the S-wave  $K\pi$  system (in analogy to the  $\rho^1 \rightarrow \rho\epsilon$  decay). In this picture the  $K^*$  is expected to decay with a  $\sin^2 \theta$  distribution. Fig. 13 shows that the data also agree with an isotropic decay, so one cannot draw a firm conclusion and exclude a Deck mechanism.

In summary we observe an enhancement in the reaction  $\gamma p \rightarrow K^* K \pi p$ , the decay properties of which

are indicative of a  $1^- \phi'$  state of mass 1.9 GeV and width  $\sim .4 \text{ GeV}/c^2$ . We cannot however exclude the presence of Deck mechanism producing this effect.

D. Proton channels : the S particle

Charged protons can be identified between 20 GeV and 35 GeV. This means that there is rather low acceptance to measure a pair  $p\bar{p}$ .

1. Elastic  $p\bar{p}$

The invariant mass distribution shown in Fig. 14 shows no obvious structure. It has a total cross section of  $(20 \pm 4) \text{ nb} \pm 6 \text{ nb}$  for  $40 < E_\gamma < 70 \text{ GeV}$ .  
syst. error

2. Inclusive  $p\bar{p}$

Inclusive  $p\bar{p}$  are coming from events with at least four charged prongs. In Fig. 15a we see a clear structure centered at 1930 MeV. As shown by Fig. 15b, this structure well separates from the  $\phi$  reflexion if we plot the  $p\bar{p}$  events in the  $K^+ K^-$  hypotheses. Due to the small acceptance one cannot safely estimate the cross section.

E. Summary and conclusions

Table I summarizes our results on exclusive photoproduction.

One is left with many open questions, but it seems that there is growing evidence that several high mass recurrences are present. It could well be, as for the  $\rho^1$  (1600) which appears less distinct in the  $4\pi$  mode than in the  $2\pi$ , that some of the enhancements that we observe are resonances distorted by the presence of a large non resonant background rather than Deck type effects.

Channel	Mass MeV	Width MeV	$\sigma_{\text{nb}}$	$1^-$
$\pi^+ \pi^-$	1 600	$230 \pm 80$	$130 \pm 20$	Yes
$\rho^0 \pi^+ \pi^-$	1 600	500	$800 \pm 300$	Yes
$\omega \pi^0$	1 250	300	$\sim 1\ 000$	Yes ?
$\pi^+ \pi^- \pi^0$	1 275	100	$\sim 100$	?
$\pi^+ \pi^- \pi^0$	1 675	100	$\sim 100$	?
$\omega \pi^+ \pi^-$	1 700	500	$\sim 100$	Yes ?
$K^+ K^-$	1 750	100	Few nb	?
$K^* K \pi \rightarrow K^+ K^- \pi^+ \pi^-$	1 900	400	$60^{+30}_{-20}$	Yes ?

TABLE I

Summary on heavy vector mesons

## II. CHARM

### A. General remarks

From the threshold behaviour of the  $\gamma p \rightarrow \psi p$  cross section and using straightforward theoretical arguments<sup>5</sup> one can set a lower limit on the total cross section for charm, free and hidden, of  $\sim 200$  nb. Since  $\psi$  are mostly produced elastically<sup>6</sup>, one expects that hidden charm will only have a small contribution.

To estimate the charm cross section from our data we need the momentum distribution of the charmed particles. It is generally expected that these heavy particles originating from beam fragments will appear energetic in the lab system. Assuming we have a flat momentum distribution, we would get an average momentum of 20 GeV. We could also use a central distribution with an average Feynman  $x$  of 0 as observed in our inclusive  $\Lambda$  data. We then get an average momentum of  $\sim 10$  GeV. In this case our identifying detectors would only accept a small fraction of the charm decay products. Keeping in mind these limitations and these uncertainties, we will assume in the following discussion an average momentum of 15 GeV.

We still have to ask ourselves which fraction of the charm cross section we are triggering on. We feel that this question is probably not too serious if, as can be deduced from colliding beam results, charm events look just like ordinary events to our trigger device. Since we are triggering on about 60 % of the total cross section, we should not be missing a large fraction of charm.

### B. Electrons

Measuring the prompt electron cross section can give us a direct estimate of the total charm cross section. If we assume that the semileptonic branching ratios for D, F and charmed baryons are about the same in the neighbourhood of 10 %, the two cross sections are simply related.

However, since the electron detector is missing low energy particles, below 3 GeV, the acceptance correction is large. We thus need a model to generate the electron spectrum. We already have assumed a 15 GeV average momentum for charmed particles and for the semileptonic decay spectrum, we will use the one observed for D's at Spear.

An alternative consists in presenting the measurement in terms of the  $e/\pi$  ratio inside our acceptance to allow a straightforward comparison with the hadronic measurements.

We combine the lead glass array and the  $\gamma$  position detector information to isolate a very pure sample of electrons. The Cerenkov is also used to eliminate pions below threshold. We measure a rejection against hadrons of  $5 \cdot 10^{-4}$  with 50 % efficiency for electrons. To eliminate electrons coming from purely electromagnetic processes, we perform transverse momentum cuts and require at least four particles at the main vertex. We also veto events in which a second electron is detected.

The background given by converted  $\gamma$  from  $\pi^0$  and  $\eta$  cannot be completely eliminated, due to asymmetric pairs, but can be estimated by looking at the  $\gamma e$  mass spectrum in which one can measure a reflection of the  $\pi^0$ . In Fig. 16 one notes a clear difference between  $\gamma e^+$  prompt and  $\gamma e^-$  prompt spectra. This difference is quantitatively interpreted by the Compton contribution only present for  $e^-$ .

In table II, we summarize the interpretation of  $e^+$  and  $e^-$  prompt electrons. The hadronic background is measured by using the shape of  $E/P$  where  $E$  is the energy deposited in the lead glass and  $P$  the momentum.

Correcting for inefficiencies and acceptance, we estimate  $B\sigma = 80 \pm 20$  nb where the error is statistical. We also measure  $e/\pi \sim 5 \cdot 10^{-4}$  which is an order of magnitude higher than in hadronic reactions.

We do not see a  $K^{\mp} - e^{\pm}$  correlation due to  $D\bar{D}$  decays so that there is not compelling evidence that this excess is indeed due to charm. One could think of some effect coming for instance from inelastic Bethe Heitler<sup>7</sup>, but crude estimates show that this tends to produce peaked electrons which we eliminate. One should also realize that only 15 % of the selected electrons are genuine prompt electrons and that acceptance effects for a 15 GeV D can suppress significantly the probability to see the associated K.

In conclusion, using this method, we get an estimate of  $800 \pm 200$  nb, for the total charm cross section (the error is only statistical).

Type	Total	Converted $\gamma$	Compton	Hadron	Excess
$e^+$	1 160	640	0	320	200
$e^-$	1 390	640	230	320	200

TABLE II  
Prompt electrons

### C. D Mesons

Classical D channels,  $K^{\pm} \pi^{\mp}$ ,  $K^{\pm} \pi^{\mp} \pi^{\mp}$  etc... have a huge combinatorial background which, in the absence of some selective cuts, does not allow us to see a significant signal with a few hundred nb cross section. Due to uncertainties on the background shape and to possible shifts on the masses, we consider we can see a signal provided it corresponds to a deviation of  $\sim 2\sigma$ . With this visibility threshold and taking into account background fluctuations, we give upper limits which correspond to a  $3\sigma$  contribution from charm. In doing so, one ends up with upper limits, very similar in all these channels, of the order of 400 nb for a D of a given polarity. Obviously these limits are not very constraining and do not contradict the electron result.

In the  $K^+ \pi^-$  channel, without any cut, we observe an excess of events at the  $\bar{D}^0$  mass (Fig. 17). No significant effect is seen in  $K^- \pi^+$ . We observe that in our data, at high  $x$  (Feynman  $x$ ),  $K^+/K^- \sim 1.7$ ,  $p/\bar{p} \sim 2$ ,  $\Lambda/\bar{\Lambda} \sim 4$ , so that one can reasonably assume by analogy that a  $\bar{D}$ , incorporating a valence quark, is more copiously produced than a D. We have tried this idea by requiring that the proton coming from the charmed baryon is also detected. Most of these protons fall below the kaon threshold (18 GeV) and are signed as  $K^+$ . Fig. 18 shows the  $K^+ \pi^-$  mass distribution with an extra  $K^+$  detected but no other cut. A well centered  $\bar{D}^0$  signal, corresponding to  $3\sigma$ , is visible.

We have tried the same method on the  $K^0 \pi^+ \pi^-$  mode. In addition to the  $K^+$ , we ask for a visible mass above 3.7 GeV and an incident photon with energy above 40 GeV. A signal is clearly visible in Fig. 19 with more than three standard deviations. A fit gives a mass

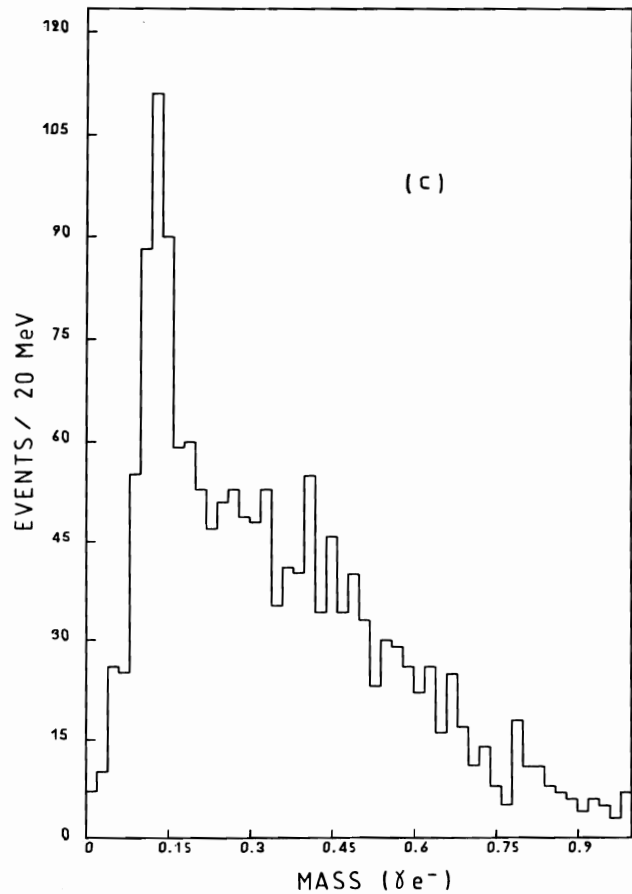
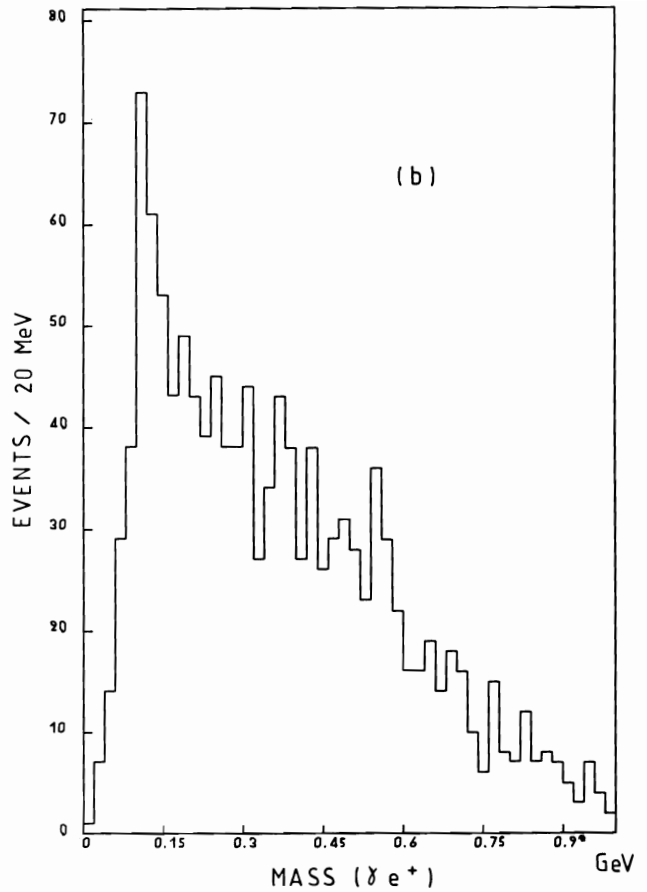
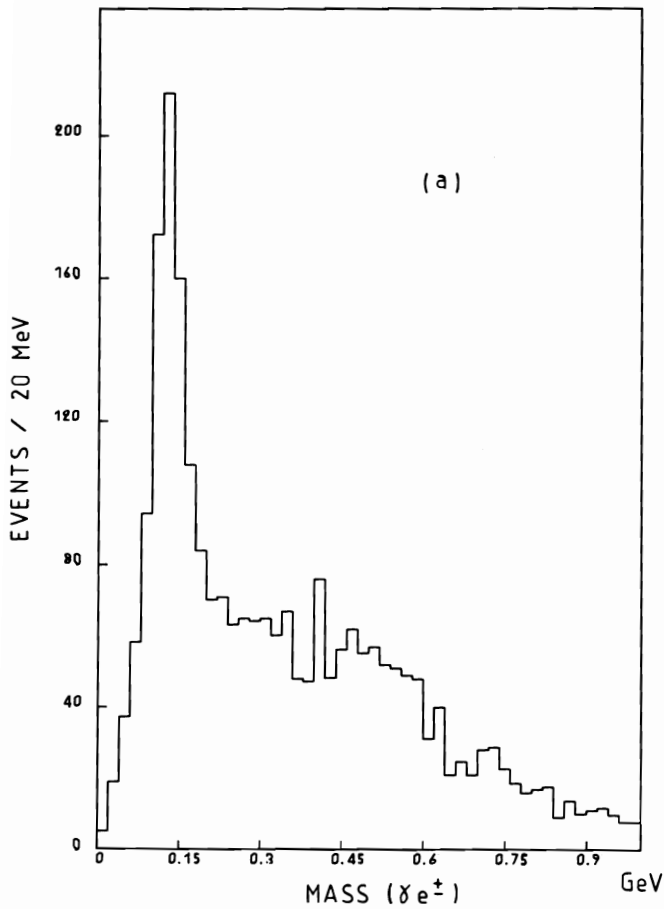


Fig. 16.  $\gamma e$  mass distributions

- (a) An asymmetric pair is identified, with one of the particles hitting the lead glass detector, the other having less than 2 GeV.
- (b) An  $e^+$  is accepted as a prompt candidate.
- (c) An  $e^-$  is accepted as a prompt candidate.

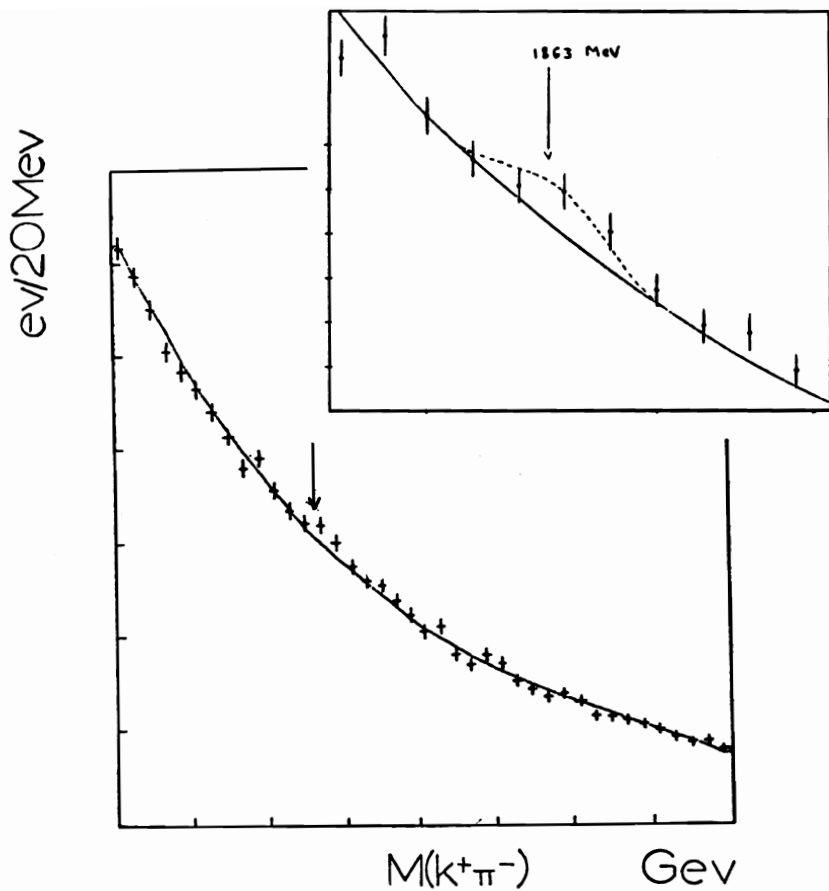


Fig. 17. Inclusive  $K^+\pi^-$  mass distribution. The curve is a polynomial fit to the data. The dotted curve in the magnified region is the expected shape for a  $D^0$  signal given our experimental resolution in that region of mass.

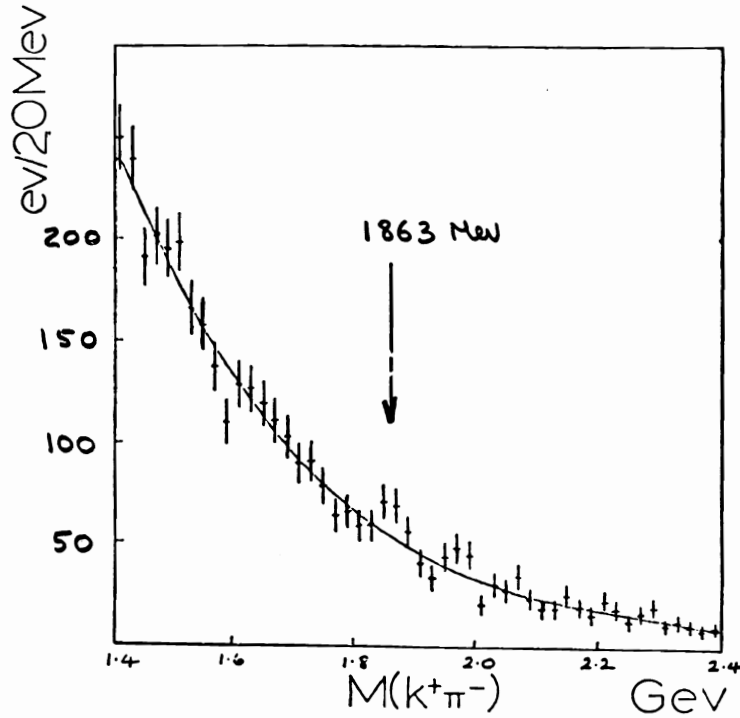


Fig. 18. Inclusive  $K^+\pi^-$  with an extra  $K^+$  (proton) in the event. The curve is a polynomial fit to the data.

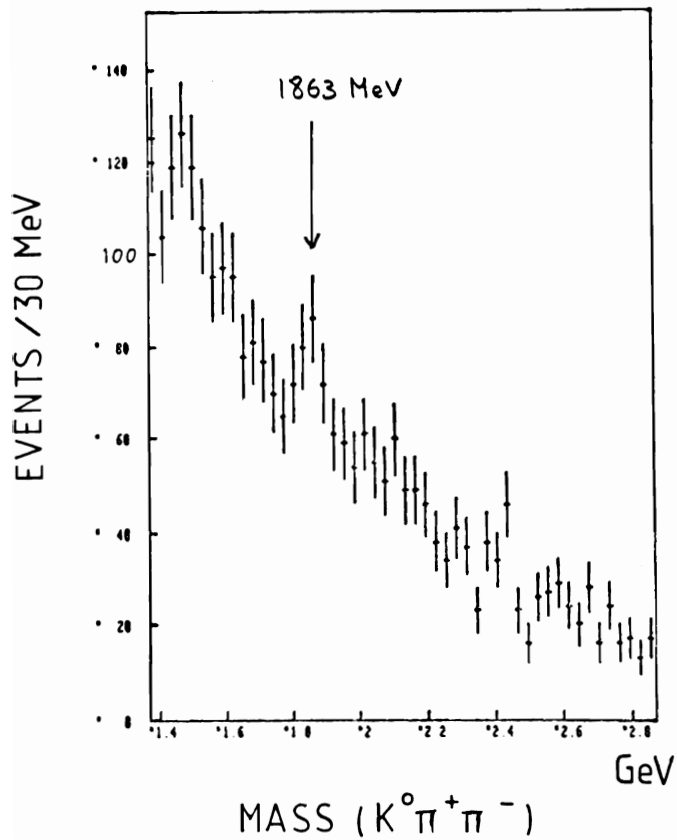


Fig. 19. Inclusive  $K_s^0 \pi^+ \pi^-$  mass distribution with the following selections :  
 - An extra  $K^+$  (proton) is seen.  
 - The total visible mass is above 3.7 GeV.  
 - The incident photon has an energy above 40 GeV.

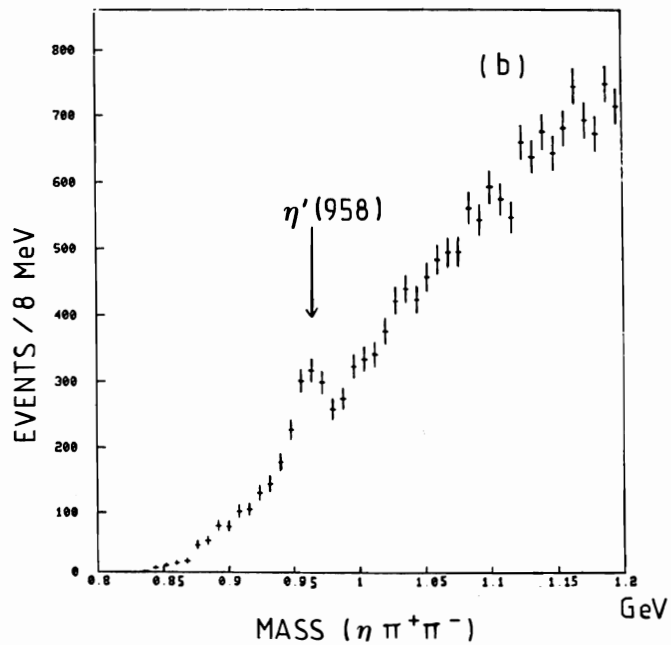
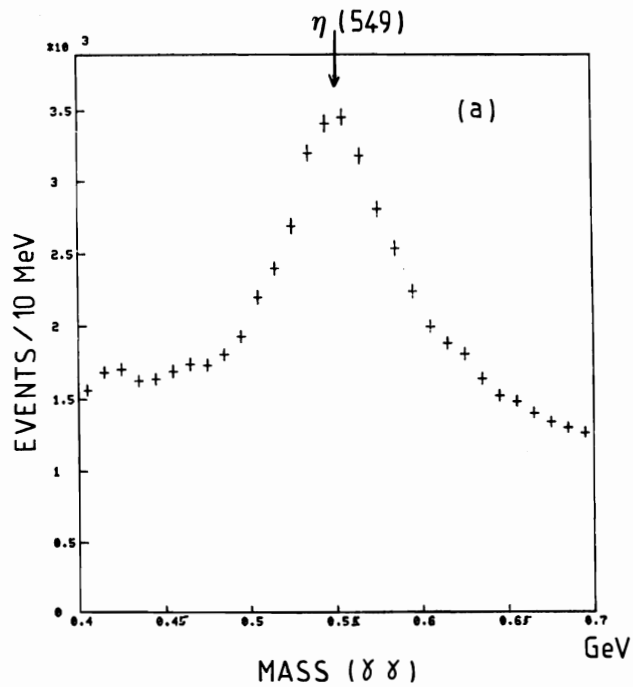


Fig. 20. (a) Inclusive  $\gamma\gamma$  mass distribution.  
 (b) Inclusive  $\eta \pi^+ \pi^-$  mass distribution.

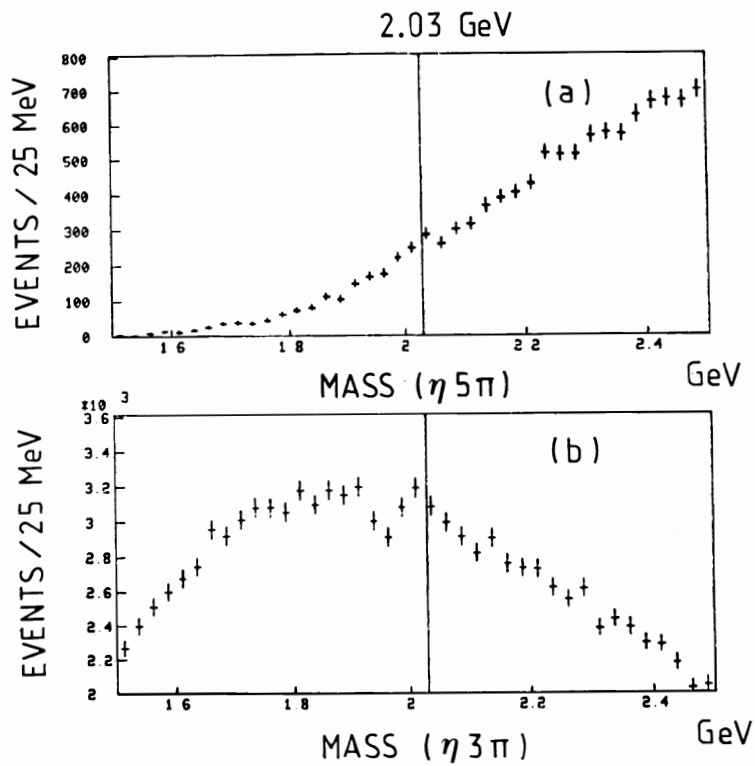


Fig. 21. (a) Inclusive  $\eta \pi^+ \pi^- \pi^+ \pi^-$  mass distribution.  
 (b) Inclusive  $\eta \pi^+ \pi^-$  mass distribution.  
 The line indicates the mass of the F found at DORIS.

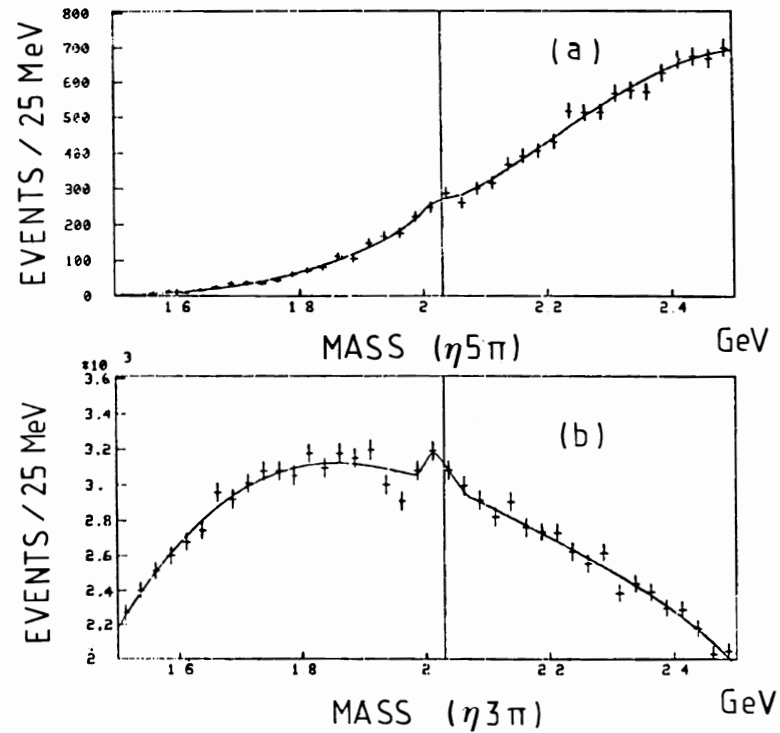


Fig. 22. (a) Inclusive  $\eta \pi^+ \pi^- \pi^+ \pi^-$  fitted mass distribution.  
 (b) Inclusive  $\eta \pi^+ \pi^-$  fitted mass distribution.  
 The fit uses a polynomial plus a gaussian.



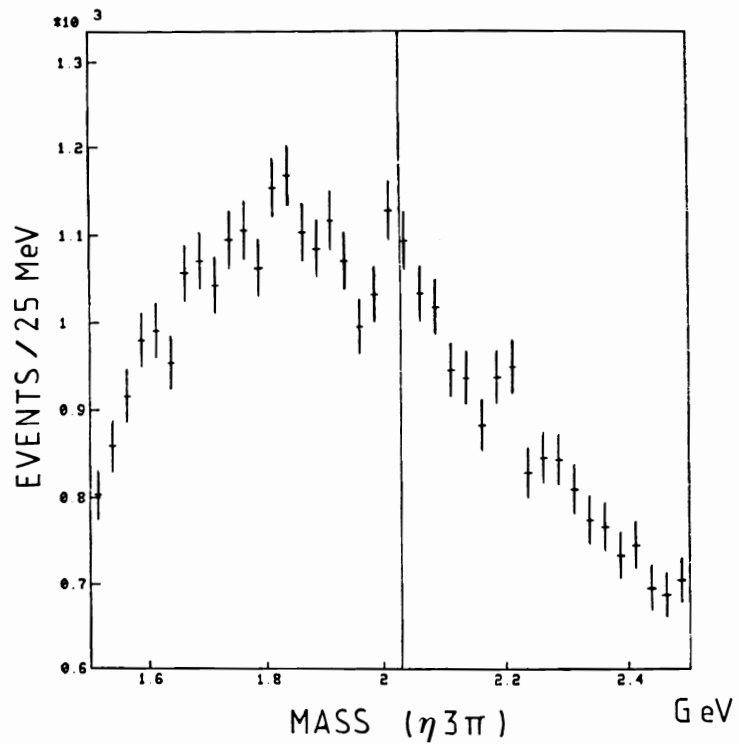


Fig. 23. Inclusive  $\eta \pi^+ \pi^-$  mass distribution requiring the presence of an extra  $\gamma$  in the event.

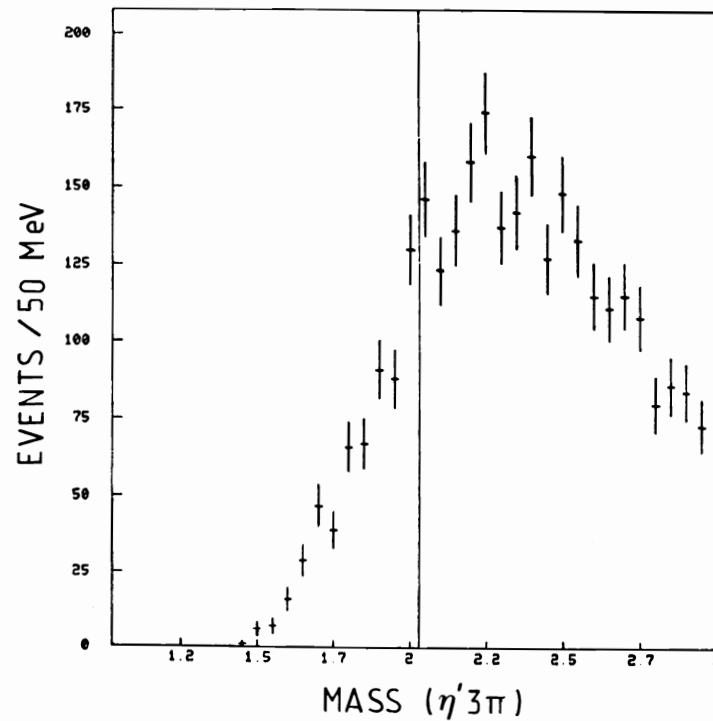


Fig. 24. Inclusive  $\eta \pi^+ \pi^- \pi^+ \pi^-$  with one  $\eta \pi^+ \pi^-$  combination consistent with the  $\eta'$  mass.

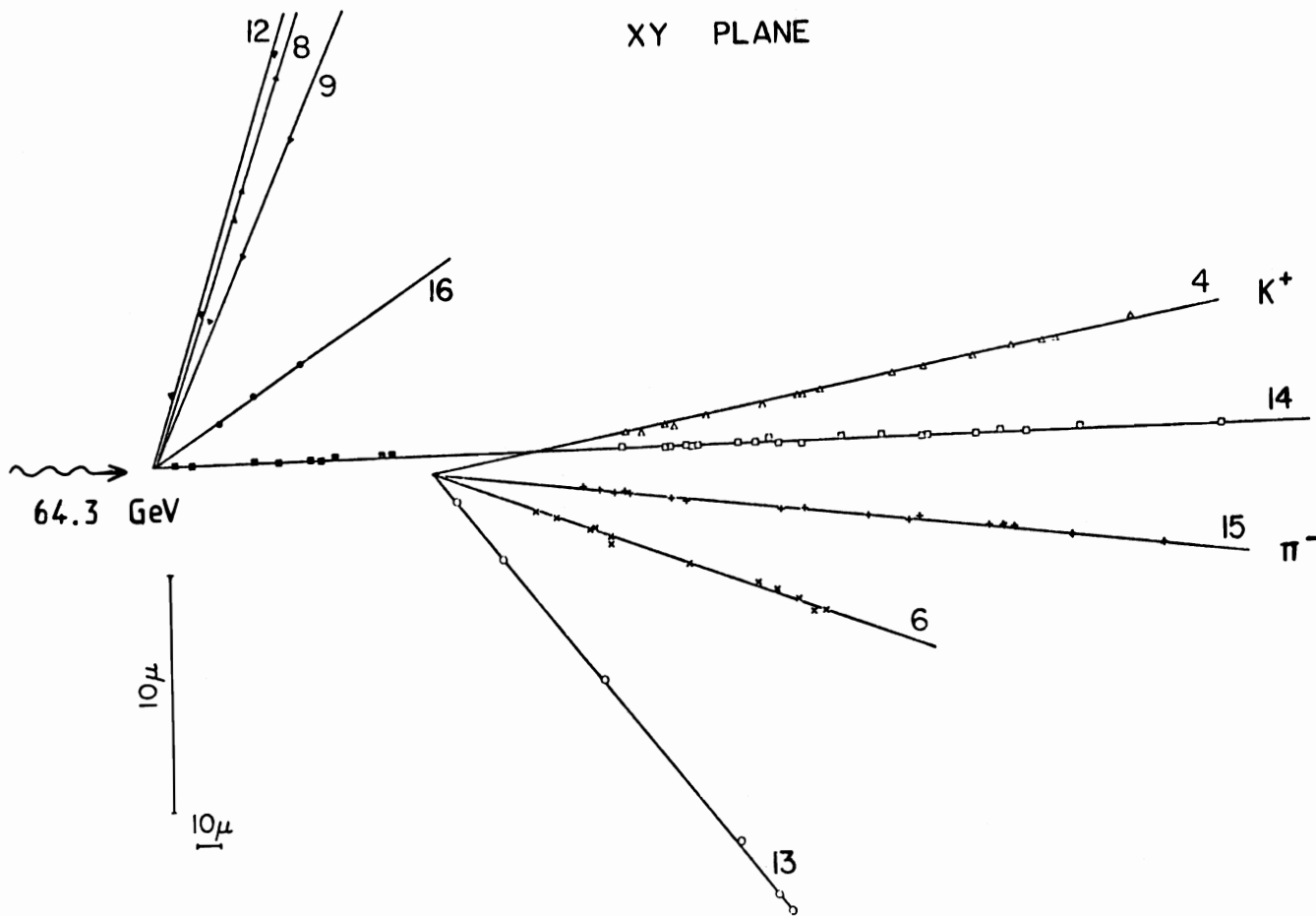


Fig. 25. Graph with the measured points (emulsion grains) and the best fit lines of all minimum ionizing tracks in emulsion. Take note of the different scale on the 2 axes.

Track 4 is identified in the Cerenkov as a  $K^+$ , track 15 as a  $\pi^-$ .

of  $1.862 \pm .013$  GeV and is consistent with the expected resolution of 60 MeV (FWHM).

#### D. F mesons

We have looked for the F in  $K^+ K^- n\pi$  channel. We find that  $B\sigma$  for the  $\phi\pi^\pm$  mode is below 20 nb.

From our photon detector, we find a sample of 14 000  $\eta$  (Fig. 20a) with a one to one signal/background ratio. This result is obtained with very mild cuts on  $\gamma$  momenta, giving us a large efficiency on  $\eta$ . On Fig. 20b, we can see a well centered  $\eta'$  in the  $\eta\pi^+\pi^-$  combinations.

In  $\eta\pi^+\pi^+$  and  $\eta\pi^+\pi^-\pi^+$ , at the mass given by DORIS, we see a  $4\sigma$  effect (Fig. 21). The width,  $\Gamma \sim 60$  MeV, is consistent with the resolution expected from an extrapolation of the  $\omega$  and  $\eta'$  experimental widths. The fit (Fig. 22) gives :

$$m(\eta 3\pi) = 2.017 \pm .011 \text{ GeV}$$

$$m(\eta 5\pi) = 2.020 \pm .007 \text{ GeV}$$

If we ask that there is an extra  $\gamma$ , the  $\eta 3\pi$  signal is seen more clearly (Fig. 23). This  $\gamma$  may originate from the  $F^*$  cascade, but also from an  $\eta$  from the partner F.

If we demand an  $\eta'$  in the  $\eta 5\pi$  system, the evidence is also improved as shown in Fig. 24. We estimate that more than 50 % of the  $\eta 5\pi$  signal is in  $\eta' 3\pi$ .

The  $\eta\pi$  spectrum shows no signal. One can speculate that this channel could have a low trigger efficiency since the F is only giving one charged prong and our trigger requires at least four charged tracks.

MODE	$B\sigma$ nb	B %	$\sigma$ nb
Inclusive e	$80 \pm 20$	10	$800 \pm 200$
$\bar{D}^0 \rightarrow K^+ \pi^-$	$5 \pm 2$	$2.0 \pm .5$	$250 \pm 100$
$\bar{D}^0 \rightarrow K^0 \pi^+ \pi^-$	$25 \pm 16$ $- 8$	$4 \pm 1.3\%$ (Mark I) $2 \pm .8\%$ (Mark II)	$600 \pm 400$ $200$ $1200 \pm 800$ $400$
$D^0 \rightarrow K^- \pi^+$	$< 7$	$2.0 \pm .5$	$< 350$
$D^\pm \rightarrow K^\mp \pi^\pm \pi^\pm$	$< 15$	$3.0 \pm .8$	$< 500$
$F \rightarrow \eta 3\pi$	$30 \pm 20$ $- 10$	10 (?)	$300 \pm 200$ $- 100$
$F \rightarrow \eta 5\pi$	$10 \pm 7$ $- 3$	?	
$F \rightarrow \eta\pi$	$< 5$	?	
$F \rightarrow \phi\pi$	$< 20$	?	

TABLE III : Summary on charm

Note : Except when there is a substantial difference with previous results, we use Mark II values for branching ratios. The errors on the branching ratios are not incorporated in our results.

#### E. Charm with emulsions

The emulsion experiment uses the set up described for WA4. Each emulsion is exposed to a flux of  $10^6$  incident photons. The pellicles,  $15 \times 15 \times .06$  cm<sup>3</sup>, were inclined at an angle of  $11^\circ$  with respect to the beam so that an emulsion thickness of 3 mm was crossed by the photons. An event can be recognized unambiguously by matching the vertices and the angles measured in the spectrometer and in the emulsion. The angular accuracies are  $\pm .5^\circ$  in azimuth and  $\pm 1^\circ$  in dip.

An event with secondary vertex of four tracks at a distance of  $(123.0 \pm 2.2)$  microns from the center of the star and at  $(.8 \pm .08)$  microns from the nearest tracks is shown in Fig. 25. It has the following characteristics :

- all forward minimum ionizing tracks are matched to  $\Omega$  tracks.

- two of the secondaries are identified as  $K^+$  and  $\pi^-$ . Assuming the other two are pions, one gets an invariant mass of  $1866 \pm 8$  MeV and a total momentum of  $33.8 \pm .2$  GeV.

- the missing transverse momentum for these secondaries is compatible with 0.

- the decay time of the system is  $(2.26 \pm .04) 10^{-14}$  sec.

The main background contribution comes from high energy  $K^0$  interactions. The probability that such effect could be due to an interaction of a secondary  $K^0$  is below  $10^{-6}$ , given that 1 000 hadronic events have been found.

The missing partner to the  $\bar{D}^0$  could be decaying in a neutral mode. This assumption is compatible with the missing mass of the star, which is a little larger than 2 GeV.

#### F. Summary and conclusions

In table III are summarized the various cross section estimates and limits obtained for charm. We feel that there is no internal inconsistency provided that what we have called the visible part of the charm cross section lies between 500 nb and  $1 \mu\text{b}$  and that F particles are as copiously produced as D particles. Our data also suggest that D should be more copiously produced than  $\bar{D}$ .

In summary, the WA4 experiment has given evidence for new vector meson recurrences. It has also given an estimate of the charm photoproduction cross section through observation of prompt electron and  $\bar{D}^0$  production. Evidence has been given for F production in two new modes. The emulsion experiment has, for the first time, observed the decay of a  $\bar{D}^0$  and reconstructed its mass.

#### REFERENCES

1. For details of the Omega spectrometer and the tagging system see D. Aston et al., to be published in Nucl. Phys. B.
2. See, for example, International Symposium on Lepton and Photon Interactions at High Energies, ed. Gutbrod (Hamburg 1977) and references therein.
3. R. Anderson et al., Phys. Rev. D1, 27 (1970).
4. J. Ballam et al., Nucl. Phys. B76, 375 (1974).

5. D. Sivers, J. Townsend and G. West, Phys. Rev. D13, 1234 (1976).
6. U. Camerini et al., Phys. Rev. Lett. 35, 483 (1975)
7. S.D. Drell and J.D. Walecka, Ann. Phys. (N.Y.) 28, 18 (1964).

#### DISCUSSION

P. NEMETHY, L.B.L.

On your table of cross sections, you assumed 15 GeV for your momentum. Just how sensitive are you to that? You said you were very sensitive. What happens to that table if you went down to 10 GeV?

F. RICHARD, L.A.L.

I would say that if I went down to 10 GeV all cross sections (except the  $K^0 \pi^+ \pi^-$  where we can have good acceptances at low energies because soft  $K^0$ 's are well detected) would go up by roughly a factor of 2.

P. NEMETHY, L.B.L.

On your emulsion event, you gave a time after the mass. Is that the proper life of that?

F. RICHARD, L.A.L.

Yes, I was too fast. Sorry. I come back to that. The flight of this secondary vertex is of order 120 microns. Since this  $D^0$  is very fast, 34 GeV, taking the gamma factor into account, we get  $2.26 \cdot 10^{-14}$  s.

J. SACTON, Brussels

There was a time when your emulsion colleague reported events in the emulsion with lifetime of the order of  $10^{-15}$  s. Are those events still alive?

F. RICHARD, L.A.L.

Perhaps they should answer?

G. DIAMBRINI-PALAZZI, Univ. of Genova

We reported at the Tokyo Conference the two events with a  $10^{-15}$  s lifetime. One was a trident with 1 electron, low energy electron, so it could be interpreted at first sight as semi-leptonic decay. Then from a measurement which is quite difficult with such a low quality emulsion that we got, we detect a second electron. So this trident has now 2 electrons so the charmed interpretation is ruled out. I mean the trident is there but could not be interpreted any more as charmed decay. The other one, 15 micron from the main vertex with an error  $\pm 5$  microns, is still there, but is uncertain due to the systematical error in the determination of the vertex position, as we already said in the Tokyo Conference.

U. NAUENBERG, Colorado

With respect to your emulsions event, you quote a probability of  $10^{-6}$  that the track is a  $K^0$ . Shouldn't you really give the ratio of the probabilities that the K have a large momentum as compared to the charmed particle having such a large momentum? In that case, what theory do you use to know what the probability for charm is?

F. RICHARD, L.A.L.

That's the main uncertainty but it's clearly much more probable for 2 GeV charmed objects coming from the photon, if you believe usual models, to have 30 GeV

from an incident photon of 60 GeV than for  $K^0$  which is very soft. We measured the inclusive  $K^0$  distribution. It's very peaked at low x. We don't know what the D distribution is, but it is a heavy object originating from the photon and thus should be fast. But we cannot prove that. In your approach, the ratio of probabilities can be slightly higher than  $10^{-6}$  but nevertheless very depressed.

A. CONTI, Florence Univ.

About the problem of the evaluation of the background for the emulsion event. In the paper presented at the conference we quoted first of all  $10^{-2}$ .  $10^{-2}$  is the most conservative of the worst probability you may have. It just takes into account the fact of having a white star with the right number of prongs. But as Richard already pointed out you may continue and take into account the fact that this supposed  $K^0$  should have half the energy. It is more than half the energy of the incident gamma. That's the second point. The third one is taking into account this mass range between 1800 and 1900 GeV. In that case, you go down to  $10^{-6}$ . But if you want the worst probability estimate, if only a white star with four prongs is  $10^{-2}$ , not taking into account any momentum and any mass.

M.J. TANNENBAUM, Rockefeller Univ.

The question is about the 2.03 bump. You showed several distributions that were like  $4\sigma$ . But I couldn't understand whether they were dependent or independent, so my question is how significant is your bump at 2.03 GeV and is it so-called F?

F. RICHARD, L.A.L.

If you don't require anything more, that means if you just take the raw data without requiring an  $\eta'$  in the  $\eta 5\pi$  or an extra gamma, etc... my answer comes from this plot. You make a fit to your data with the polynomial background and you put a Breit Wigner or a Gaussian, it doesn't matter, in that region. And you find that roughly the significance for the  $\eta 5\pi$  is  $3.7 \sigma$  and for the  $\eta 3\pi$  is of the order of  $4\sigma$ . You have the same mass in the 2 systems.

M.J. TANNENBAUM, Rockefeller Univ.

So these are totally independent?

F. RICHARD, L.A.L.

Yes, they are totally independent. That's the strong point, I think.

D. YENNIE, Cornell

I'd like to make a comment about the 4 pion mass distribution. This is really an elaboration of Truong's remark. It could be that the interfering background is much stronger than the resonance itself and that there's a somewhat narrower resonance at about 1700 or 1800 MeV, which has a constructive interference below and a destructive interference above, which gives the appearance of a rather broad resonance at about 1600. This is somewhat supported by the electroproduction experiments because it's our general understanding that as  $Q^2$  increases, this interfering Drell type background tends to decrease more rapidly than the resonance peak itself. This is shown in the  $\rho$  electroproduction. So it could be that the same resonance that's showing up from the electroproduction experiment at Cornell could influence the photoproduction experiment by giving this constructive interference on one side and destructive on the other.

F. RICHARD, L.A.L.

Do you say that the background is the same in  $e^+e^-$  than in photoproduction ?

D. YENNIE, Cornell

No, it wouldn't have to be the same. It could be that the background is relatively larger in photoproduction in the same way that it is in the Drell process.

F. RICHARD, L.A.L.

I have tried to use the fit for  $e^+e^-$  in  $4\pi$  and it fits nicely our data. So I would tend to believe that we see the same thing.

D. YENNIE, Cornell

It could be, yes.

V. LUTH, SLAC

What's the kind of confidence you get from the fit in the neighbourhood of the  $\eta 3\pi$  peak. I mean I see the deviation as large as  $4\sigma$  in the neighbourhood of that peak.

F. RICHARD, L.A.L.

I think you are referring to the fact that these points are low.

V. LUTH, SLAC

Exactly. And the ones right below these low points are far above.

F. RICHARD, L.A.L.

You are saying these points are low and where do you see high points ?

V. LUTH, SLAC

One doesn't. I just wonder what the confidence of that fit is in the neighbourhood of that peak. If you don't go quite 100 MeV away in the background, but if you stay close.

F. RICHARD, L.A.L.

You mean if I just take a narrow region of mass, what happens around the F ? Well that was my first attempt in the first transparency I have shown where I just tried to make a local fit. This is of course a very coarse local fit. The significance doesn't change dramatically. It's of the order of  $4\sigma$  as well. Maybe that answers your question, I'm not sure.